Journal of Molecular Structure 1062 (2014) 125–132

Contents lists available at ScienceDirect

Journal of Molecular Structure

journal homepage: www.elsevier.com/locate/molstruc

Synthesis, structure, terahertz spectroscopy and luminescent properties of copper(I) complexes with mercaptan ligands and triphenylphosphine

Qi-Ming Qiu [a], Min Liu [b], Zhong-Feng Li [a], Qiong-Hua Jin [a,*], Xu Huang [a], Zhen-Wei Zhang [c], Cun-Lin Zhang [c], Qing-Xuan Meng [a,d]

[a] *Department of Chemistry, Capital Normal University, Beijing 100048, China*
[b] *The College of Materials Science and Engineering, Beijing University of Technology, Beijing 100022, China*
[c] *Beijing Key Laboratory for Terahertz Spectroscopy and Imaging, Key Laboratory of Terahertz Optoelectronics, Ministry of Education, Department of Physics, Capital Normal University, Beijing 100048, China*
[d] *Daxing High School Attached to CNU, Beijing 102600, China*

HIGHLIGHTS

- Seven new complexes were synthesized and characterized.
- Complexes **1**–**5** represent first examples of HMNBT and HAMTD with copper(I) halides.
- The complexes **1**, **5**, **6** and **7** exhibit interesting fluorescence in the solid state.
- THz-TDS of starting materials and complexes were investigated.
- Our results show several factors can affect the THz spectra of the complexes.

ARTICLE INFO

Article history:
Received 24 July 2013
Received in revised form 28 December 2013
Accepted 28 December 2013
Available online 8 January 2014

Keywords:
Copper(I) halides
Triphenylphosphine
Mercaptan ligands
Luminescence
Terahertz spectroscopy

ABSTRACT

The reactions of copper(I) halides with triphenylphosphine (PPh_3) and mercaptan ligand [2-mercapto-6-nitrobenzothiazole (HMNBT), 2-amino-5-mercapto-1,3,4-thiadiazole (HAMTD) and 2-mercapto-5-methyl-benzimidazole (MMBD)] yielded seven complexes, $[CuCl(HMNBT)(PPh_3)_2]$ (**1**), $[CuX(HMNBT)(PPh_3)]_2$ (X = Cl, Br) (**2**–**3**), $[Cu(MNBT)(HMNBT)(PPh_3)_2]$ (**4**), $[CuBr(HAMTD)(PPh_3)_2]\cdot CH_3OH$ (**5**) and $[CuX(MMBD)(PPh_3)_2]\cdot 2CH_3OH$ (X = Br, I) (**6**–**7**). These complexes were characterized by elemental analysis, X-ray diffraction, ^1H NMR and ^{31}P NMR spectroscopy. In these complexes the mercaptan ligands act as monodentate or bridged ligand with S as the coordination atom. In complexes **1** and **4**, hydrogen bonds $C—H\cdots X$ and weak interactions $C—H\cdots\pi$ lead to the formation of chains and 2D network respectively, while complexes **2** and **3** are dinuclear. In **5**–**7**, intramolecular hydrogen bonds link the $[CuX(thione)(PPh_3)_2]$ molecules and the solvated methanol molecules into centrosymmetric dimers. Complexes **1**–**5** represent first copper(I) halide complexes of HMNBT and HAMTD. The complexes **1**, **5**, **6** and **7** exhibit interesting fluorescence in the solid state at room temperature and their terahertz (THz) time-domain spectroscopy was also studied.

1. Introduction

Copper(I) is an important metal ion, which has a strong tendency to form covalent bonds with ligands containing sulphur or phosphorus donor atoms. Copper(I) complexes containing triphenylphosphine (PPh_3) and heterocyclic mercaptan ligands have received much attention in the past, mainly because of their interesting coordination chemistry [1] and potential applications in biochemistry [2], photography [3] and enzymatic reactions [4].

In previous literature, the mercaptan ligands have been known as co-ligands in forming mono or dinuclear Cu(I)-PPh_3 complexes. There are mainly two types of structures for this kind of complexes: the first kind is like $[CuX(thione)(PPh_3)_2]$ (X = Cl, Br, I) [5] and $[Cu(\mu\text{-}X)(thione)(PPh_3)]_2$ [6], where the mercaptan ligands act as a monodentate ligand with the S atom as a coordination atom; the second kind is like $[CuX(\mu\text{-}S)(thione)(PPh_3)]_2$ [7], where the mercaptan ligands act as a bridged thiol. Apart from these mono or dinuclear Cu(I)-PPh_3 complexes, Safin and Klein have also synthesized a series of Cu(I) clusters containing PPh_3 and mercaptan ligands [8,9]. The luminescence properties of the Cu(I) halide aggregates have been also investigated in recent years [10]. Che and his co-workers have prepared several d^{10} metal complexes

---

* Corresponding author. Tel.: +86 10 68903033; fax: +86 10 68902320.
E-mail address: jinqh@mail.cnu.edu.cn (Q.-H. Jin).

0022-2860/$ - see front matter © 2014 Elsevier B.V. All rights reserved.
http://dx.doi.org/10.1016/j.molstruc.2013.12.076

which exhibit emissive $\pi-\pi_*$ IL (intraligand) charge-transfer excited states by utilizing the "donor–acceptor" type ligand [3a]. Gdaniec and his co-workers also investigate the luminescence properties of Cu(I) compounds. The [CuX(L)(PPh_3)$_2$] compounds show intense luminescence in both the solid state and in solution, which originates probably from mixed LMCT/LLCT transitions [11].

Terahertz time-domain spectroscopy (THz-TDS) is a vibrational spectroscopic technique that is used to probe the infrared active vibrational modes in the far-infrared and sub-millimeter region of the electromagnetic spectrum by measuring the ultrashort pulses of coherent terahertz radiation (0.1–4 THz) (3–133 cm^{-1}). Compared with conventional spectroscopic techniques, THz-TDS has a high signal-to-noise ratio. This spectroscopic technique also enables the characterization of solid-state materials through the excitation of soft intramolecular vibrational modes, intermolecular modes, and hydrogen-bonding modes. In regard to border security, the inspection and identification of contraband drugs using terahertz TDS could be an additional tool of great significance [12]. Although THz-TDS has been utilized in a wide range of research fields in the past ten years, including chemical and biological detections and identifications [13], this technique is seldom used for organic/inorganic compounds and inorganic–organic hybrid. So, in this work, some complexes were characterized by THz-TDS.

We focus our attention on Cu(I) complexes with different heterocyclic mercaptan ligands containing PPh_3, aiming to gain insight into the interplay between the ligand's characteristics and the structural diversity observed. We also want to investigate the effect of halide ions, PPh_3, heterocyclic mercaptan ligands as well as hydrogen bonds on luminescence properties. The three mercaptan ligands 2-mercapto-6-nitrobenzothiazole (HMNBT), 2-amino-5-mercapto-1,3,4-thiadiazole (HAMTD) and 2-mercapto-5-methyl-benzimidazole (MMBD) are capable to coordinate with metal atoms (Scheme 1) because they all contain a —SH group and potential coordination N atoms, and their amino or imino group may form intramolecular and intermolecular hydrogen bonds with other acceptors [14–16]. These free ligands can exhibit fluorescence signal and the emission band may shift after their coordinating to the Cu(I) atom in complexes. The strong electron-withdrawing substituent (—NO_2) on the phenyl in HMNBT ligand and the electron-donating substituent (—CH_3) on the phenyl in MMBD ligand may also affect the structure and luminescence property of the complexes. Furthermore, to our best knowledge, only one literature have reported the Cu(I) complex with HMNBT, HAMTD and MMBD [17].

In light of these facts, we thought it was worthwhile to study Cu(I) complexes of PPh_3 with HMNBT, HMNBT and MMBD, especially their luminescence properties. The Cu(I) complexes are often prepared in acetonitrile and dichloromethane [18], but these seven Cu(I) complexes were synthesized in the mixture of methanol and dichloromethane. In this paper, terahertz time-domain spectra of four copper(I) complexes (**1**, **5**–**7**) and their starting materials (including PPh_3, mercaptan ligands and copper salts) were measured, and found that their effective signals are in the range from 0.2 to 1.6 THz. The above results are supplement of spectroscopy, our results show the anions, ligands, coordination and hydrogen bond interactions can affect the THz spectra of the Cu(I) complexes.

2. Experimental

2.1. Materials and measurements

All chemical reagents are commercially available and used without further purification. Elemental analyses (C, H, N) were determined on a Vario EL elemental analyzer. Infrared spectra were recorded on a Nicolet Avatar 360 FT-IR spectrometer using the KBr pellet in the range of 400–4000 cm^{-1}. Excitation and emission spectra of the solid samples were recorded on an F-4500 fluorescence spectrophotometer at room temperature. ^1H NMR was recorded at room temperature with a Varian VNMRS 600 MHz spectrometer and ^{31}P NMR was recorded at room temperature with a Bruker DPX 400 MHz spectrometer. The THz absorption spectra were recorded on the THz time domain device of Capital Normal University of China, based on photoconductive switches for generation and electro-optical crystal detection of the far-infrared light. The experimental apparatus for terahertz transmission measurements has been discussed in detail elsewhere [19]. The preparation of the samples is by pressing the pure crystals into pellet. The detection of THz absorption spectra is carried out at N_2 atmosphere to avoid the influence of water vapor. The thick of the samples **1**, **5**, **6**, **7** and ligands are about 1 mm. The THz absorption spectra of the samples are obtained by the THz time-domain device and the effective spectrum range is 0.2–1.6 THz.

2.2. Synthesis of complexes *1*–*7*

Compound **1**: A mixture of CuCl (0.0198 g, 0.2 mmol) and HMNBT (0.0424 g, 0.2 mmol, HMNBT = 2-mercapto-6-nitrobenzothiazole) in MeOH and CH_2Cl_2 (10 mL, v/v = 1:1) was stirred for 2 h and PPh_3 (0.1049 g, 0.4 mmol) was added to the mixture which was stirred for further 4 h. The insoluble residues were removed by filtration, and the filtrate was evaporated slowly at room temperature for a week to yield orange crystalline products. Compounds **2**–**3** was prepared in a manner similar to that described for **1,** using CuCl (0.0198 g, 0.2 mmol) or CuBr (0.0287 g, 0.2 mmol), HMNBT (0.0424 g, 0.2 mmol) and PPh_3 (0.0525 g, 0.2 mmol) as starting materials. After three days, orange crystals were formed. Compound **4**: using CuSCN (0.0243 g, 0.2 mmol), HMNBT (0.0424 g, 0.2 mmol), PPh_3 (0.0525 g, 0.2 mmol) as starting materials. After three days, orange crystals were formed. Compound **5**: using CuBr (0.0287 g, 0.2 mmol), HAMTD (0.0266 g, 0.2 mmol, HAMTD = 2-amino-5-mercapto-1,3,4-thiadiazole), PPh_3 (0.1049 g, 0.4 mmol) as starting materials. After a week, colorless crystals were formed. Compounds **6**–**7**: using CuBr (0.0287 g, 0.2 mmol) or CuI (0.0381 g, 0.2 mmol), MMBD (0.0328 g, 0.2 mmol, MMBD = 2-mercapto-5-methyl-benzimidazole), PPh_3 (0.1049 g, 0.4 mmol) as starting materials. After a week, colorless crystals were formed (see Scheme 2).

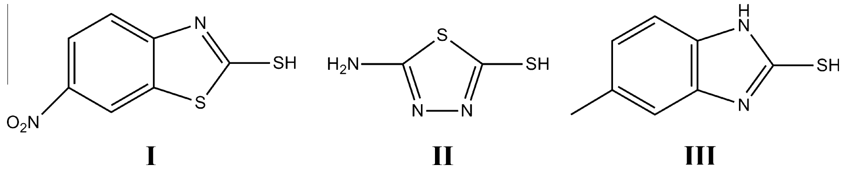

Scheme 1. The molecular structures of three mercaptan ligands, I–III for 2-mercapto-6-nitrobenzothiazole (HMNBT), 2-amino-5-mercapto-1,3,4-thiadiazole (HAMTD) and 2-mercapto-5-methyl-benzimidazole (MMBD).

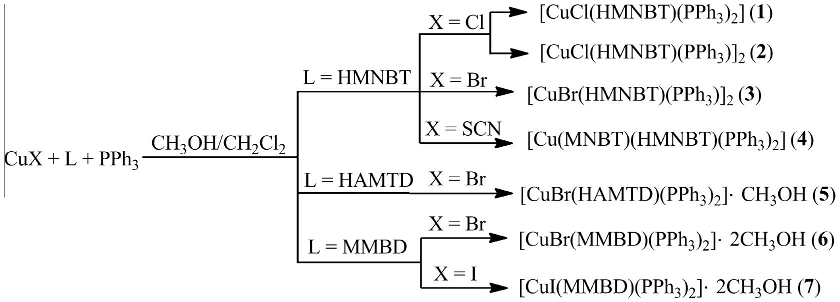

PPh_3 = triphenylphosphine HMNBT = 2-mercapto-6-nitrobenzothiazole

HAMTD = 2-amino-5-mercapto-1,3,4-thiadiazole MMBD = 2-mercapto-5-methyl-benzimidazole

Scheme 2. The routine of synthesis for complexes **1**–**7**.

2.3. Crystal structure determination and refinement

The X-ray single crystal data collections for the seven complexes were performed on a Bruker SMART CCD diffractometer with graphite monochromatized Mo Kα radiation ($\lambda = 0.71073$ Å). Semi-empirical absorption corrections were applied. The structures were solved by direct methods and refined by the full-matrix least-squares method on F^2 using the SHELXS 97 and SHELXL-97 programs [20,21]. All non-hydrogen atoms in the complexes were refined anisotropically. The hydrogen atoms were generated geometrically and treated by a mixture of independent and constrained refinements.

3. Results and discussion

3.1. General aspects

Seven Cu(I) complexes were characterized by elemental analysis, X-ray diffraction, IR, ^1H NMR and ^{31}P NMR spectroscopy, the data are listed below. A summary of the crystallographic data and details of the structural refinements are listed in Table 1. Selected bond distances and bond angles are listed in Tables S1–S4.

[CuCl(HMNBT)(PPh_3)$_2$] (**1**), Mr: 835.77. $Z = 2$. Yield: 88%. Mp: 250–252 °C. Anal. Calc. for $C_{43}H_{34}ClCuN_2O_2P_2S_2$: C, 61.74; H, 4.07; N, 3.35. Found: C, 61.51; H, 3.97; N, 3.39%. IR (KBr disc, cm^{-1}): 3435m, 3052m, 2498m, 1602m, 1584m, 1530s, 1484vs, 1433s, 1397m, 1363w, 1334vs, 1301m, 1265s, 1183m, 1158w, 1134m, 1093s, 1054s, 1026s, 997m, 890w, 873w, 836m, 743s, 693vs, 657m, 517s, 498s, 462m, 425w. ^1H NMR (600 MHz, $CDCl_3$, 298 K): $\delta = 7.2$–7.4 (m, overlapping with the solvent signal, Ph + HMNBT-Ph), 8.2 (d, 1H, HMNBT-Ph), 8.3 (s, 1H, HMNBT-Ph) ppm. ^{31}P NMR (400 MHz, $CDCl_3$, 298 K): $\delta = -2.4$ (s, PPh_3) ppm.

[CuCl(HMNBT)(PPh_3)]$_2$ (**2**), Mr: 1147.00. $Z = 1$. Yield: 23%. Mp: 241–244 °C. Anal. Calc. for $C_{50}H_{38}Cl_2Cu_2N_4O_4P_2S_4$: C, 52.31; H, 3.31; N, 4.88. Found: C, 51.99; H, 3.27; N, 4.74%. IR (KBr disc, cm^{-1}): 3437w, 3053m, 2758w, 2499m, 1678vw, 1602m, 1584m, 1530s, 1484vs, 1433s, 1397m, 1363w, 1334vs, 1302s, 1265s, 1183m, 1158w, 1134m, 1094s, 1054s, 1026s, 997m, 890w, 873w, 837m, 744s, 693vs, 657m, 618w, 542vw, 517s, 499s, 462m, 425w. ^1H NMR (600 MHz, $CDCl_3$, 298 K): $\delta = 7.2$–7.4 (m, overlapping with the solvent signal, Ph + HMNBT-Ph), 8.2 (d, 1H, HMNBT-Ph), 8.3 (s, 1H, HMNBT-Ph) ppm. ^{31}P NMR (400 MHz, $CDCl_3$, 298 K): $\delta = -2.0$ (s, PPh_3) ppm.

[CuBr(HMNBT)(PPh_3)]$_2$ (**3**), Mr: 1235.92. $Z = 1$. Yield: 25%. Mp: 253–254 °C. Anal. Calc. for $C_{50}H_{38}Br_2Cu_2N_4O_4P_2S_4$: C, 48.55; H,

Table 1
Crystallographic data for complexes **1**–**7.**

Complex	**1**	**2**	**3**	**4**	**5**	**6**	**7**
Formula	$C_{43}H_{34}ClCuN_2O_2P_2S_2$	$C_{50}H_{38}Cl_2Cu_2N_4O_4P_2S_4$	$C_{50}H_{38}Br_2Cu_2N_4O_4P_2S_4$	$C_{50}H_{37}CuN_4O_4P_2S_4$	$C_{39}H_{36}BrCuN_3OP_2S_2$	$C_{46}H_{46}BrCuN_2O_2P_2S$	$C_{46}H_{46}CuIN_2O_2P_2S$
Crystal system	Triclinic	Triclinic	Triclinic	Monoclinic	Monoclinic	Monoclinic	Monoclinic
Space group	$P\bar{1}$	$P\bar{1}$	$P\bar{1}$	$P2_1/c$	$P2_1/c$	$P2_1/c$	$P2_1/c$
a (Å)	9.6892(8)	9.2301(9)	9.2716(8)	12.3106(11)	13.0137(5)	12.7732(13)	12.8018(11)
b (Å)	13.5820(13)	10.6540(10)	10.6403(9)	36.653(3)	16.3117(7)	18.4028(18)	18.6030(19)
c (Å)	15.9842(15)	13.4181(12)	13.4775(13)	11.1401(10)	18.3089(10)	18.7296(19)	18.7696(16)
α (°)	89.987(2)	86.300(2)	86.985(2)	90.00	90.00	90.00	90.00
β (°)	72.8710(10)	70.1020(10)	70.1970(10)	111.8630(10)	100.5590(10)	92.4710(10)	93.0850(10)
γ (°)	80.0090(10)	87.997(2)	87.848(2)	90.00	90.00	90.00	90.00
V (Å^3)	1976.8(3)	1238.0(2)	1248.94(19)	4665.1(7)	3820.7(3)	4398.5(8)	4463.5(7)
Z	2	1	1	4	4	4	4
$F(000)$	860	584	620	2080	1700	1848	1920
Reflections collected	9960	6215	6269	23,579	13,996	21,833	22,101
Independent reflections	6868	4289	4312	8227	6736	7752	7752
Goodness-of-fit on F^2	1.027	1.013	1.013	1.034	1.028	1.019	1.072
R_{int}	0.0331	0.0235	0.0271	0.0861	0.0366	0.0436	0.0501
$R_1[I > 2\sigma(I)]$	0.0471	0.0367	0.0385	0.0534	0.0598	0.0377	0.0410
$wR_2[I > 2\sigma(I)]$	0.1047	0.0848	0.0832	0.0854	0.1347	0.0820	0.0868
R_1 (all data)	0.0889	0.0570	0.0677	0.1072	0.0963	0.0693	0.0801
wR_2(all data)	0.1322	0.0993	0.0968	0.0959	0.1582	0.0960	0.1144

3.07; N, 4.53. Found: C, 48.91; H,3.10; N, 4.49%. IR (KBr, cm^{-1}): 3437m, 3052m, 2968m, 2888m, 2820m, 2714m, 1604m, 1582w, 1521s, 1475vs, 1433s, 1393s, 1334vs, 1302s, 1250s, 1179ww, 1132w, 1095w, 1051m, 1023s, 997w, 900w, 838m, 821m, 746s, 694s, 674m, 654w, 552w, 520s, 507m, 491m, 458m. ^{1}H NMR (600 MHz, CDCl$_3$, 298 K): δ = 7.2–7.6 (m, overlapping with the solvent signal, Ph + HMNBT-Ph), 8.3–8.4 (m, 2H, HMNBT-Ph) ppm. ^{31}P NMR (400 MHz, CDCl$_3$, 298 K): δ = −2.4 (s, PPh$_3$) ppm.

[Cu(MNBT)(HMNBT)(PPh$_3$)$_2$] (**4**), Mr: 1011.56. *Z* = 4. Yield: 15%. Mp: 222–223 °C. Anal. Calc. for $C_{50}H_{37}CuN_4O_4P_2S_4$: C, 59.31; H, 3.66; N, 5.54. Found: C, 60.00; H, 3.61; N, 5.62%. IR (KBr disc, cm^{-1}): 3435m, 3051m, 2095vw, 1606w, 1586w, 1569w, 1529w, 1529m, 1480m, 1433s, 1396m, 1366m, 1331vs, 1312vs, 1272s, 1122m, 1092m, 1048m, 1028m, 1003s, 880w, 836m, 822m, 740s, 691s, 647m, 512s, 488m, 465m, 425w. ^{1}H NMR (600 MHz, CDCl$_3$, 298 K): δ = 7.2–7.6 (m, overlapping with the solvent signal, Ph + HMNBT), 8.3–8.4 (m, 4H, HMNBT), 10.8 (s, 1H, HMNBT-NH) ppm. ^{31}P NMR (400 MHz, CDCl$_3$, 298 K): δ = −2.4 (s, PPh$_3$) ppm.

[CuBr(HAMTD)(PPh$_3$)$_2$]·CH$_3$OH (**5**), Mr: 832.22. *Z* = 4. Yield: 69%. Mp: 233–235 °C. Anal. Calc. for $C_{39}H_{36}BrCuN_3OP_2S_2$: C, 56.24; H, 4.32; N, 5.05. Found: C, 56.30; H, 4.27; N, 5.00%. IR (KBr disc, cm^{-1}): 3398m, 3238m, 3137m, 3053m, 2905m, 1606s, 1552vs, 1480s, 1433vs, 1350m, 1312m, 1183w, 1094s, 1051s, 1027s, 998m, 856vw, 743vs, 695vs, 618w, 582w, 544w, 516s, 491m, 432w. ^{1}H NMR (600 MHz, CDCl$_3$, 298 K): δ = 4.8 (s, 2H, HAMTD-NH$_2$), 7.2–7.5 (m, overlapping with the solvent signal, PPh$_3$-Ph) ppm. ^{31}P NMR (400 MHz, CDCl$_3$, 298 K): δ = −4.3 (s, PPh$_3$) ppm.

[CuBr(MMBD)(PPh$_3$)$_2$]·2CH$_3$OH (**6**), Mr: 896.30. *Z* = 4. Yield: 74%. Mp: 287–288 °C. Anal. Calc. for $C_{46}H_{46}BrCuN_2O_2P_2S$: C, 61.59; H, 5.13; N, 3.12. Found: C, 61.77; H, 5.04; N, 3.04%. IR (KBr disc, cm^{-1}): 3393m, 3050s, 1671m, 1615m, 1585w, 1514s, 1479vs, 1434vs, 1382m, 1322m, 1224w, 1182m, 1094s, 1027m, 997w, 857w, 801m, 743s, 694vs, 629w, 594vw, 545w, 515s, 493m, 425w. ^{1}H NMR (600 MHz, CDCl$_3$, 298 K): δ = 2.4 (s, 3H, MMBD-CH$_3$), 7.0–7.1 (m, 3H, MMBD-Ph), 7.2–7.4 (m, overlapping with the solvent signal, PPh$_3$-Ph), 10.9 (d, 2H, MMBD-NH) ppm. ^{31}P NMR (400 MHz, CDCl$_3$, 298 K): δ = −4.2 (s, PPh$_3$) ppm.

[CuI(MMBD)(PPh$_3$)$_2$]·2CH$_3$OH (**7**), Mr: 943.29. *Z* = 4. Yield: 89%. Mp: 293–295 °C. Anal. Calc. for $C_{46}H_{46}ICuN_2O_2P_2S$: C, 58.52; H, 4.88; N, 2.97. Found: C, 58.44; H, 4.90; N, 2.99%. IR (KBr disc, cm^{-1}): 3400 m, 3176s, 3053s, 1963w, 1891w, 1816w, 1668w, 1615 m, 1585 m, 1571w, 1510 m, 1476vs, 1433vs, 1383 m, 1319s, 1222 m, 1183 m, 1092s, 1025 m, 998 m, 921vw, 852w, 804 m, 741s, 692vs, 626 m, 594 m, 543 m, 507s, 425w. ^{1}H NMR (600 MHz, CDCl$_3$, 298 K): δ = 2.4 (s, 3H, MMBD-CH$_3$), 7.0–7.1 (m, 3H, MMBD-Ph), 7.2–7.4 (m, overlapping with the solvent signal, PPh$_3$-Ph), 10.6 (d, 2H, MMBD-NH) ppm. ^{31}P NMR (400 MHz, CDCl$_3$, 298 K): δ = −5.3 (s, PPh$_3$) ppm.

Generally, the Cu(I) complexes of halides with triphenylphosphine (PPh$_3$) are prepared in acetonitrile and dichloromethane [18]. In our work, these Cu(I) complexes were synthesized at room temperature in the mixture of methanol and dichloromethane mainly because the crystal of good quality could be obtained. The coordination properties of the mercaptan ligand and PPh$_3$ towards the Cu(I) precursors CuX (X = Cl, Br, I) were investigated. The Cu(I) metal centre is coordinated by the soft P donor atoms and the soft S donor atoms, which help to stabilize the lower oxidation state of Cu atom.

It's should be mentioned that molar ratio and solvent are important to the formation of the title compounds. The direct reaction of copper(I) halides with mercaptan ligand and PPh$_3$ in 1:1:2 M ratio yield the complexes **1**, **5**–**7**, and the dinuclear complexes **2** and **3** are formed by the reaction of CuX (X = Cl, Br) with HMNBT and PPh$_3$ in 1:1:1 M ratio. It is interesting that in complex **4**, the HMNBT ligand is connected to the nitrogen atom of the deprotonated HMNBT molecule by hydrogen bond, and the thiocyanate anion is substituted by the deprotonated mercaptan ligand.

To obtain the full series of this type of complexes, we studied the reactions of CuX (X = Cl, Br, I, SCN) with three mercaptan ligand and PPh$_3$ in the molar ratio 1:1:1 or 1:1:2 in the mixed solvent of CH$_2$Cl$_2$ and CH$_3$OH. Except the reactions which produce the seven title compounds and [CuI(MMBD)(PPh$_3$)$_2$]·CH$_3$OH [17], the other reactions were failed and many of them only produced the adducts CuX:PPh$_3$. The possible reason is that anions induce PPh$_3$ substitutes mercaptan ligand in the Cu(I) complexes.

As regards to the IR spectra, the absorptions in the 3437–3393 cm^{-1} region are attributed to υ(NH) stretching frequencies for complexes **1**–**4** and **6**–**7**. In complex **5**, the stretching at 3398 cm^{-1} and 3238 cm^{-1} is attributed to ligand's —NH$_2$ group. The absorptions around 3053 cm^{-1} are caused by the C—H stretching vibration of the phenyl ring in all the complexes. The υ(C═S) bands are located at 856–801 cm^{-1}, showing that the ligands bind the metal via the sulfur atoms [22,23]. The typical absorptions around 512 cm^{-1} in all the complexes are due to the Cu—P bonds [24].

The ^{1}H NMR and ^{31}P NMR spectra of complexes **1**–**7** have been measured at room temperature in CDCl$_3$ solution. The ^{1}H NMR spectra of complexes **4**, **6** and **7** exhibit the signal of NH group at 10.8 ppm, 10.9 ppm and 10.6 ppm, respectively. The lack of the signal of the NH group in the ^{1}H NMR spectra of complexes **1**–**3** shows that the ligand is deprotonated in the solution. For complexes **1**–**7**, the resonance signals in the range of 7.0–8.4 ppm are assigned to the protons of PPh$_3$ and the mercaptan ligand. The broad multiplet signals of aromatic protons of PPh$_3$ for **1**–**7** are in the range of 7.2–7.4 ppm, 7.2–7.4 ppm, 7.2–7.6 ppm, 7.2–7.5 ppm, 7.2–7.5 ppm, 7.2–7.4 ppm and 7.2–7.4 ppm, respectively. For **1**–**4**, the multiple signals at range 8.20–8.45 ppm are assigned to 2-mercapto-6-nitrobenzothiazole protons. For **5**, the signal of NH$_2$ in 2-amino-5-mercapto-1,3,4-thiadiazole ligand is at 4.78 ppm. In ^{1}H NMR spectra of complex **6**–**7**, there is a multiplet in the range 7.0–7.1 ppm, which is assigned to benzimidazole protons. There is a singlet at 2.4 ppm in **6**–**7**, which is attributed to methyl protons of benzimidazole. In ^{31}P NMR spectra of **1**–**7**, all phosphorus atoms in each molecule are chemically equivalent because only a single resonance signal is found (−2.4 ppm for **1**, −2.0 ppm for **2**, −2.4 ppm for **3**, −2.5 ppm for **4**, −4.3 ppm for **5**, −4.2 ppm for **6**, −5.3 ppm for **7**). The similarity of resonance signals in solution of **1**–**7** show that the chemistry environment for the phosphorus atom from PPh$_3$ in **1**–**7** is similar.

3.2. Crystal structures of the complexes

*3.2.1. [CuCl(HMNBT)(PPh$_3$)$_2$] (**1**)*

The perspective view of **1** is shown in Fig. 1. The Cu(I) atom is coordinated by two phosphorus atoms from two PPh$_3$ ligands, one chloride atom and one sulfur atom from HMNBT. The Cu—S bond distance [2.414(1) Å] and Cu—P bond distances [2.266(1)–2.270(1) Å] are similar to those reported in other copper(I) complexes [25–27]. The bond angles around Cu atom ranging from 98.5(1)° to 131.2(1)° are similar to those of the previously reported similar complex [25]. The tetrahedral distortion may be attributed to steric interactions between the bulky phosphine ligands, which is common among a large series of monomeric Cu(I) halide complexes containing one heterocyclic thione and two monodentate PPh$_3$ ligands [25,27–29]. The S—Cu—Cl angle is almost the same as those in other similar complexes, this is due to the existence of the strong intramolecular N—H···Cl [174(1)°] hydrogen bond of chlorine atom with the imino hydrogen in its vicinity [N1···Cl1, 3.001 Å]. The chain is generated via weak C28—H28···Cl1 bond [C28···Cl1, 3.605(6) Å] formed by the chloride atom and the C—H group of PPh$_3$ ligand (Fig. S1 in the

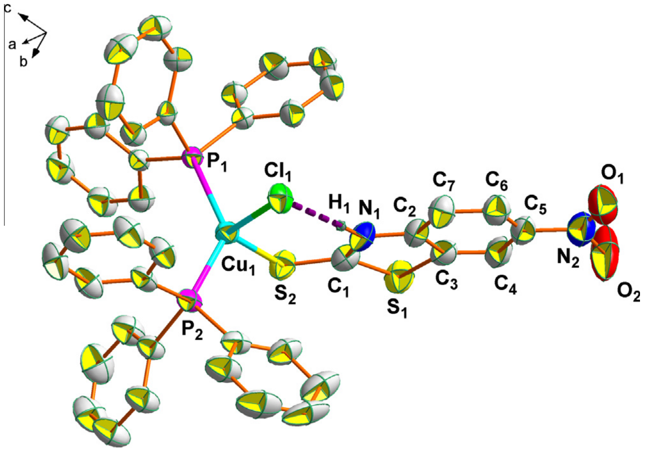

Fig. 1. The molecular entities of complex **1**. Thermal ellipsoids drawn at the 50% probability level. The intramolecular hydrogen bonds N—H···Cl are shown with dashed lines. Omit all of the other H-atoms not involved in H-bonding.

Supporting information), and weak C—H···π interactions (C29—H29···Ph, 2.86 Å) involving phenyl groups of two different phosphines. There is also a weak π interaction between the O1 atom and the C2—C7 ring (by using PLATON software), which explain the difference in the shape of O1 and O2 (the ellipsoid for O2 is elongated whereas O1 is regular).

3.2.2. [CuX(HMNBT)(PPh$_3$)]$_2$ (X = Cl, Br) (**2**–**3**)

The perspective view of **2** and **3** are shown in Fig. 2. The basic structural units of **2** and **3** are dimer in which the two copper atoms are doubly bridged by two S atoms of the thione ligand to form a strict planar four-membered Cu_2S_2 core. The Cu···Cu distances are 2.832(1) and 2.805(1) Å in **2** and **3**, respectively. These values are slightly longer than the sum of van der Waals radii of two copper atoms (2.80 Å) [30]. The Cu—P bond distances in **2** [2.239(1) Å] and **3** [2.244(1) Å] are slightly shorter than the corresponding distances in complex **1**. The two non-equivalent Cu—S bond distances are 2.349(1) and 2.494(1) Å in **2**, and 2.340(1) and 2.506(1) Å in **3**, which are within the range expected for dinuclear Cu(I) complexes with double bridging sulfur atoms [28,31]. The angles of S(2)#1-Cu(1)—S(2) [108.5(1)°] and Cu(1)#1-S(2)—Cu(1) [71.5(1)°] are not equal, the sum of the internal angles of the four-membered ring [—Cu—S—Cu—S—] in the Cu_2S_2 core are approximately 360°, which indicates that the ring is a parallelogram. In complex **2**, the centroid to centroid distance between the benzothiazole ring and benzene ring is 3.784(2) Å with the dihedral angle of 5.5°, which suggests the existence of π···π interactions between them [complex **3**: 3.766(2) Å, 6.3°]. Furthermore, intramolecular hydrogen bonds N—H···Cl and N—H···Br are also observed [N1···Cl1 = 3.096(3) Å, N1—H1···Cl1 = 157(1)°; N1···Br1 = 3.247(4) Å, N1—H1···Br1 = 153(1)°].

3.2.3. Cu(MNBT)(HMNBT)(PPh$_3$)$_2$ (**4**)

In complex **4**, two phosphorus atoms from two triphenylphosphines, two sulfur atoms from the neutral ligand HMNBT and the deprotonated ligand MNBT are coordinated to the Cu(I) cation (Fig. 3). The N—H group of the HMNBT ligand is connected to the nitrogen atom of the MNBT ligand by the hydrogen bond N—H···N [N1···N3 = 2.817(4) Å, N1—H1···N3 = 168(1)°]. This mode of intramolecular association between MNBT and HMNBT leads to the formation of an eight-membered ring. It is interesting that the thiocyanate anion in complex **4** is successfully substituted by the mercaptan ligand. The structure of complex **4** is the first authenticated example with the coordinated neutral HMNBT ligand. Furthermore, intramolecular N—H···S hydrogen bond is also observed [N1···S4 = 3.540(4) Å, N1—H1···N3 = 125(1)°]. It is noticeable that O4 atom is connected to another HMNBT ligand via C4—H4···O4 hydrogen bond to form the chain (Fig. S2). In complex **4**, the centroid to centroid distance between parallel adjacent benzene rings of HMNBT ligand is 3.654(2) Å, which suggests the existence of π···π interactions between them. The chains interact with each other via π···π interactions and weak C—H···π interactions (C13—H13···Ph, 2.84 Å) involving phenyl groups of two different phosphines to form the network structure (Fig. S3).

3.2.4. [CuBr(HAMTD)(PPh$_3$)$_2$]·CH$_3$OH (**5**), [CuX(MMBD)(PPh$_3$)$_2$]·2CH$_3$OH (X = Br, I) (**6**–**7**)

The molecular structures of **5**–**7** are similar, and complexes **6** and **7** are isostructural. HAMTD and MMBD act as neutral, monodentate ligand with the S atom as a coordination atom. Other sites of the coordination tetrahedron are occupied by two P atoms from two PPh_3 ligands and one halide anion (Figs. S4 and S5). As in similar Cu(I)-PPh_3 complexes, the environment around copper(I) is distorted tetrahedral, the P—Cu—P angle between the triphenylphosphine ligands in **5**–**7** varies between 121.5(1)° and 122.0(1)° [25]. The arrangement of the mercaptan ligand within the complex is dictated by the intramolecular N—H···X hydrogen bond. In **5**–**7**,

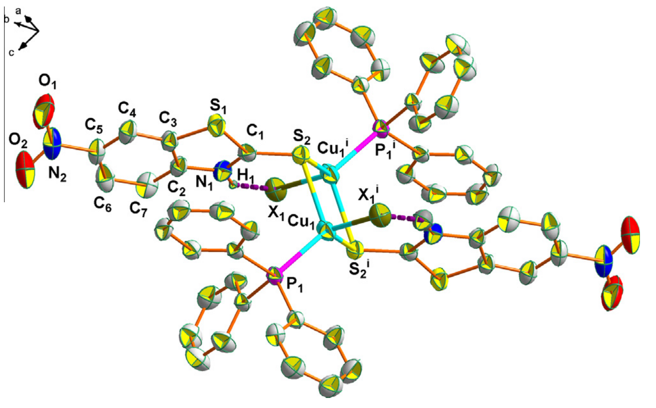

Fig. 2. The molecular entities of complexes **2**–**3**. Thermal ellipsoids drawn at the 50% probability level. The intramolecular hydrogen bonds N—H···X are shown with dashed lines. Omit all of the other H-atoms not involved in H-bonding.

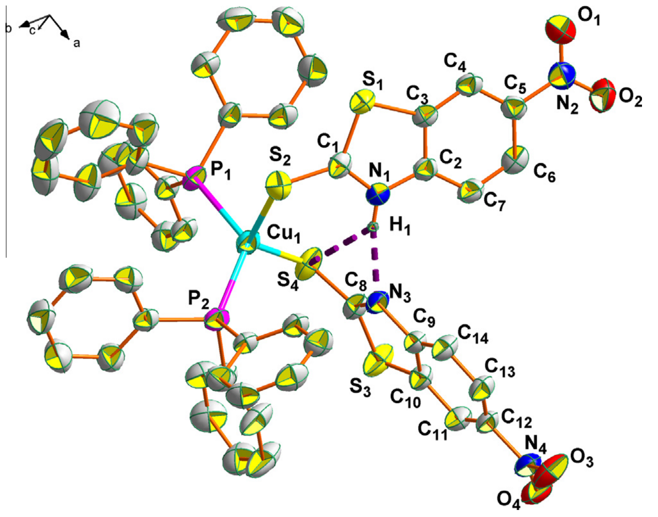

Fig. 3. The molecular entities of complex **4**. Thermal ellipsoids drawn at the 50% probability level. The intramolecular hydrogen bonds N—H···N and N—H···S are shown with dashed lines. Omit all of the other H-atoms not involved in H-bonding.

a dimer is formed by hydrogen bonds N—H···X, O—H···X and O—H···O between the unit [CuX(thione)$(PPh_3)_2$] and the solvent methanol molecules. In complex **6**, the centroid to centroid distance between the benzothiazole ring and benzene ring is 3.553(2) Å with the dihedral angle of 0.4°, which suggests the existence of π···π interactions between them [complex **7**: 3.511(3) Å, 0.8°].

3.3. Discussion of the crystal structures

In the seven title Cu(I) complexes, the Cu^I ion as a metal center adopts tetrahedral coordination geometry when the coordination number is four. In complexes **1**–**2**, the ligand HMNBT plays different roles: the HMNBT in complex **1** acts as a monodentate ligand with the S atom as a coordination atom, while the mercaptan ligand in complex **2** acts as a bridged thiol. The different roles of HMNBT are possibly due to the different molar ratio of the reactants. Complex **1** and **2** are formed by the reaction of CuCl with HMNBT and PPh_3 in molar ratios 1:1:2 and 1:1:1 respectively. It is interesting that in the reaction of **4** the thiocyanate anion is successfully substituted by the mercaptan ligand. The structure of complex **4** is the first authenticated example containing coordinated neutral HMNBT ligand. The results show that SCN^- may be substituted easier than Cl^-/Br^- anion. It is noticeable that C—H···O hydrogen bonds, C—H···π interactions and π···π interactions lead to the formation of 2D networks in complex **4**, which may be due to the existence of conjugated system and strong electron-withdrawing group ($-NO_2$) in HMNBT ligand and the inexistence of halides ions in **4**. However, the solvent methanol molecules in complexes **5**–**7** lead to the formation of a dimer. In complexes **6**–**7**, due to the existence of a phenyl group in the ligand MMBD, there are intermolecular π···π interactions between benzothiazole ring and benzene rings which help to stabilize the dimer. Furthermore, the isostructure of **2** and **3**, **6** and **7** shows that the anions Cl^-, Br^- and I^- do not affect the final structures.

3.4. Luminescence

The excitation and emission spectra of free ligands HMNBT, HAMTD and MMBD, and the complexes **1**, **5**, **6** and **7** are measured in the solid state at room temperature (Fig. 4). The ligand PPh_3 exhibits fluorescence signal centered at 402 nm with an excitation maximum at 370 nm. Free mercaptan ligands were excited at the same excitation wavelength of 439 nm, and found that the emission maximum are exhibited at 467, 552 (HMNBT); 468, 539 (HAMTD); and 469, 546 nm (MMBD), respectively. In the fluorescence emission spectra of **1**, **5**, **6** and **7**, the emission peaks are found at 405, 468, 568 nm ($\lambda_{ex} = 340$ nm for **1**), 395, 475 nm ($\lambda_{ex} = 244$ nm for **5**), 396, 507 nm ($\lambda_{ex} = 344$ nm for **6**), 394, 478 nm ($\lambda_{ex} = 339$ nm for **7**), respectively. Emission peaks of the above complexes around 400 nm are similar to that of PPh_3, which indicates that the origin of these emissions involves emissive state derived from ligand-centered [π–π^*] transition. Absorption maxima at around 300 nm and emissions around 450–510 nm are typical of Cu—P containing chromophores with either ILCT (σ-a_π); MLCT (d-σ_*) excited states [32].

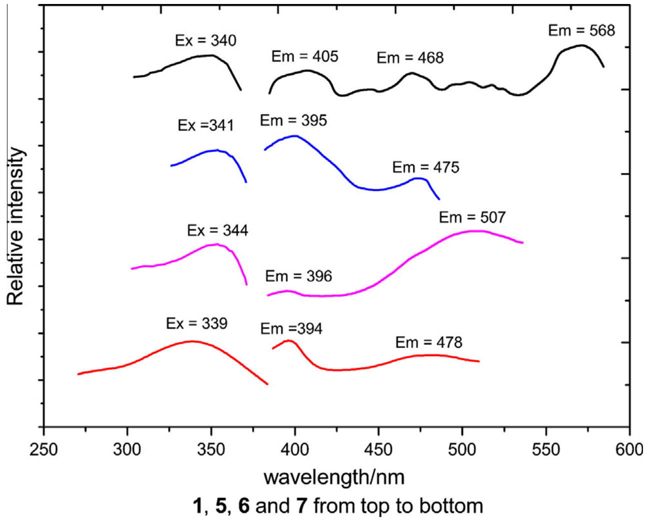

Fig. 4. The luminescent excitation and emission spectra of **1**, **5**–**7** in the solid state at room temperature.

It is interesting that the solid sample of **1** exhibits an intense low-energy emission with λ_{em} at 568 nm, which is slightly red-shifted with respect to the free mercaptan ligand HMNBT. But for **5**–**7**, no emission peak appears in the range of 520–600 nm. Among these four complexes, **1** is un-solvated while **5**–**7** are methanol-solvated. In **5**–**7**, the O—H group of solvated methanol molecules forms hydrogen bonds O—H···X and O—H···O with other atoms, which may cause the quenching of the low-energy emission peak.

Although the slight red shift in **1** and **6**–**7** are considered as evidence for participation of Cu → S charge transfer in the emissive excited state since the Cu^I ion express strong tendency for charge transfer of this type, the emissions cannot be considered as one of pure thione centred intraligand origin [11,33,34]. The halogen could affect the emission spectra, in the form of a ligand-to-metal charge-transfer (XMCT) or an interligand charge-transfer (XLCT, X → thione) [35]. There is a small dependence of the emission maxima on the kind of the halide present, the λ_{max} values of complexes **6** and **7** are in the order **7** < **6**, which is consistent with the order of ligand field strength of the halide ions in the complexes ($I^- < Br^-$) [36,37]. From the above results, we can conclude that PPh_3 and mercaptan ligands are sensitizers for luminescence of **1** and **5**–**7**. And the complexes **1**, **5**, **6** and **7** act as green, cyan and blue emitter component, respectively.

In summary, the determination of the emissive excited states in the Cu(I) complexes is still a difficult topic. The emissive states are most likely of mixed MLCT/XLCT/IL character. Since the luminescence properties of the Cu(I) halide aggregates have been widely investigated, the complexes might have potential applications in fluorescent sensors, electroluminescent devices and nonlinear optics [18,38,39].

3.5. THz properties of complexes

The room temperature terahertz (THz) absorption spectra of CuCl, CuBr, CuI, triphenylphosphine (PPh_3) 2-mercapto-6-nitrobenzothiazole (HMNBT), 2-amino-5-mercapto-1,3,4-thiadiazole (HAMTD), 2-mercapto-5-methyl-benzimidazole (MMBD), complexes **1** and **5**–**7** were measured in the range of 0.2–1.6 THz. All the above compounds except PPh_3 ligand have characteristic resonance peaks. The found peaks for each compound are as following: HMNBT (0.87, 1.25, 1.36 and 1.49 THz), HAMTD (0.65, 1.09, 1.18 and 1.24 THz), MMBD (0.84 and 1.08THz), complex **1** (0.69, 0.78 and 0.87 THz), complex **5** (0.89 and 1.46THz), complex **6** (1.10, 1.33 and 1.48 THz), complex **7** (1.14, 1.25 and 1.40 THz) (Fig. 5a–c). Although the agreement between crystal structure and observed spectra does not allow a definitive characterization of the spectra, it is possible to make tentative assignments of many observed features in the terahertz region for the samples. By comparing the THz absorption spectra of the products with those of the reactants, we can see that after reaction, most peaks of the mercaptan ligands and CuX disappeared or moved, and new peaks in the range of 1.25–1.48 THz appear in the obtained complexes. For example, one peak at 1.46 THz appears in the spectrum of complex

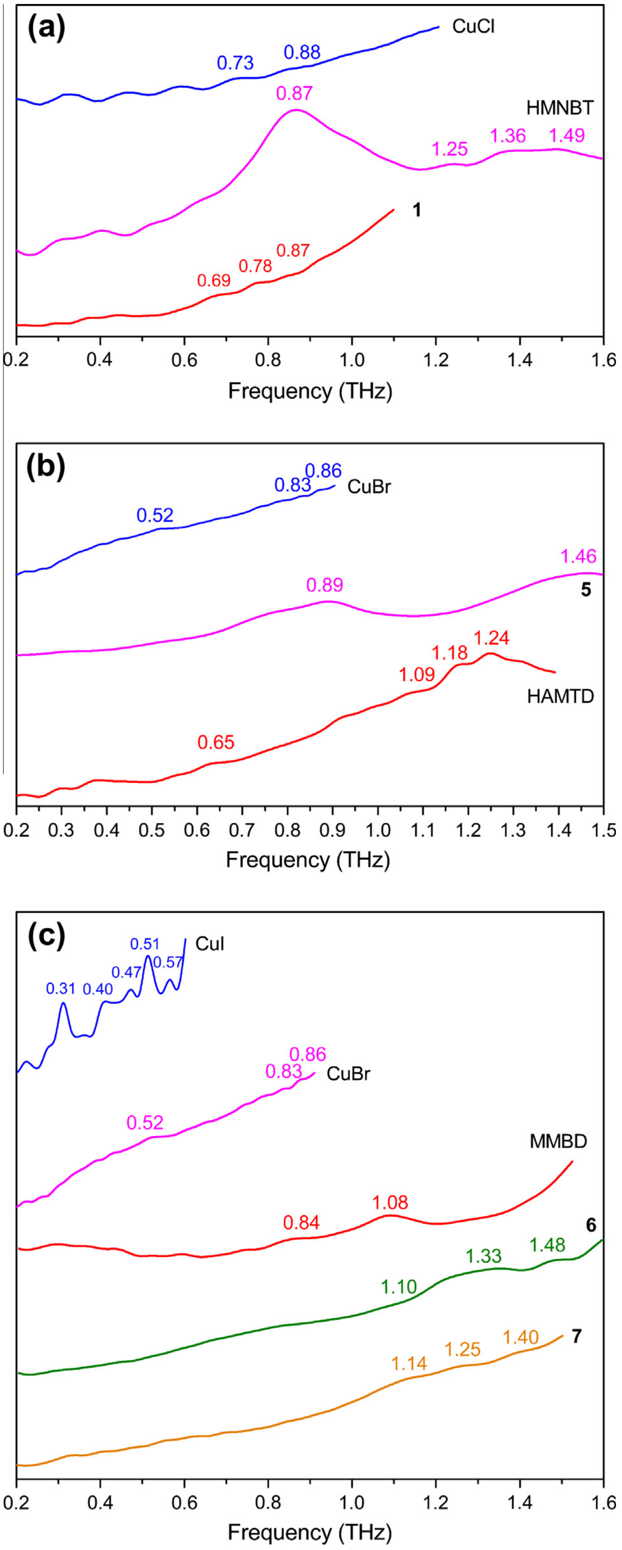

Fig. 5. (a) THz absorption spectra of CuCl, HMNBT and complex **1**. (b) THz absorption spectra of CuBr, HAMTD and complex **5**. (c) THz absorption spectra of CuBr, CuI, MMBD, and complexes **6** and **7**.

5; two new peaks at 1.33 and 1.48 THz appears in the spectrum of complex **6**; two new peaks at 1.25 and 1.40 THz appear in the spectrum of complex **7**. These changes in the THz spectra may be related to the coordination of the ligands to the Cu(I) metal atoms, and also related to the inter- or intra-molecular hydrogen bonds. It is interesting that though complexes **6** and **7** are isostructural, both of them exhibit a similar pattern of absorption features in the range 1.2–1.5 THz. In complex **7**, this pattern comprises two absorption peaks at 1.25 THz and 1.40 THz, which appear blue-shifted in complex **6** at 1.33 THz and 1.48THz. This shows that the THz spetra can distinguish Br^- from I^-, this is to say the difference of anion can affect the THz spectra of compounds. The above results show that the ligands, metal salts, the coordination and hydrogen bonding interactions can affect the THz spectrum. So THz spectroscopy may be a sensitive method to determine some of the inorganic–organic hybride complexes, especially those isostructural complexes which are difficult to identify by other spectroscopy.

4. Conclusion

Seven new Cu(I)-PPh_3 complexes of 2-mercapto-6-nitrobenzothiazole (HMNBT), 2-amino-5-mercapto-1,3,4-thiadiazole (HAMTD) and 2-mercapto-5-methyl-benzimidazole (MMBD) have been synthesized and characterized for the first time. Copper(I) atom has a strong tendency to form covalent bonds with S/P ligands and the molar ratio and solvent has played an important role in the synthesis of this series of complexes. Among these complexes, **1**–**5** represent first copper (I) examples of HMNBT and HAMTD. In complex **4**, a unique coordination mode of HMNBT was found. Complexes **1** and **5**–**7** exhibit interesting emission in the solid state. The hydrogen bond interactions may cause the quenching of the low-energy emission peak in **5**–**7**. Terahertz time-domain spectra of four Cu(I) complexes and the starting materials were measured. Our results indicate that the ligands, anions, and the metal–ligand coordination and hydrogen bonding interactions can affect the THz spectra of Cu(I) complexes. The above results may be useful in characterizing the isostructural complexes which are difficult to identify by other spectroscopy. Currently, there is not enough THz information for inorganic–organic hybrid complexes and their starting materials. Further studies on the syntheses, structures and THz properties of Cu(I) complexes with different heterocyclic ligands containing sulphur or phosphorus donor atoms are in progress.

Acknowledgements

This work has been supported by the National Natural Science Foundation of China (Grant No. 21171119), the National High Technology Research and Development Program 863 of China (Grant No. 2012AA063201), the Committee of Education of the Beijing Foundation of China (Grant No. KM201210028020), Program for Excellent Talents of Beijing City (Grant No. 2010D005016000002), the Beijing Municipal Natural Science Foundation (Grant No. 7122015).

Appendix A. Supplementary data

CCDC 890632, 892818, 890635, 893648, 890630, 890636 and 893864 contain the supplementary crystallographic data for **1**–**7**. These data can be obtained free of charge via http://www.ccdc.cam.ac.uk/conts/retrieving.html, or from the Cambridge Crystallographic Data Centre, 12 Union Road, Cambridge CB2 1EZ, UK; fax: (+44) 1223 336033; or e-mail: deposit@ccdc.cam.ac.uk.

Supplementary data associated with this article can be found, in the online version, at http://dx.doi.org/10.1016/j.molstruc.2013.12.076.

References

[1] (a) M. Gennari, M. Lanfranchi, L. Marchio, M.A. Pellinghelli, M. Tegoni, R. Cammi, Inorg. Chem. 45 (2006) 3456;

(b) H. Noth, W. Beck, K. Burger, Eur. J. Inorg. Chem. (1998) 93;
(c) T.S. Lobana, Rekha, B.S. Sidhu, A. Castineiras, E. Bermejo, T. Nishioka, J. Coord. Chem. 58 (2005) 803;
(d) G.P. Voutsas, S.C. Kokkou, C.J. Cheer, P. Aslanidis, P. Karagiannidis, Polyhedron 14 (1995) 2287;
(e) M. Belicchi-Ferrari, F. Bisceglie, E. Buluggiu, G. Pelosi, P. Tarasconi, Polyhedron 29 (2010) 2134.

[2] (a) E.S. Raper, Coord. Chem. Rev. 129 (1994) 91;
(b) D. Katiyar, V.K. Tiwari, R.P. Tripathi, A. Srivastava, V. Chaturvedi, R. Srivastava, B.S. Srivastava, Bioorg. Med. Chem. 11 (2003) 4369.

[3] (a) C.-H. Li, S.C.F. Kui, I.H.T. Sham, S.S.Y. Chui, C.-M. Che, Eur. J. Inorg. Chem. (2008) 2421;
(b) P.C. Ford, E. Cariati, J. Bourassa, Chem. Rev. 99 (1999) 3625;
(c) V.W.W. Yam, K.K.W. Lo, Chem. Soc. Rev. 28 (1999) 323.

[4] (a) P. Chen, S.I. Gorelsky, S. Ghosh, E.I. Solomon, Angew. Chem. Int. Ed. 43 (2004) 4132;
(b) Y. Lee, A.A.N. Sarjeant, K.D. Karlin, Chem. Commun. (2006) 621;
(c) E.I. Solomon, R.K. Szilagyi, S.D. George, L. Basumallick, Chem. Rev. 104 (2004) 419;
(d) J.T. York, I. Bar-Nahum, W.B. Tolman, Inorg. Chim. Acta 361 (2008) 885.

[5] (a) P. Aslanidis, S.K. Hadjikakou, P. Karagiannidis, M. Gdaniec, Z. Kosturkiewicz, Polyhedron 12 (1993) 2221;
(b) G.K. Batsala, V. Dokorou, N. Kourkoumelis, M.J. Manos, A.J. Tasiopoulos, T. Mavromoustakos, M. Simic, S. Golic-Grdadoinik, S.K. Hadjikakou, Inorg. Chim. Acta 382 (2012) 146;
(c) S. Shakhatreh, M. Lalia-Kantouri, M. Gdaniec, P.D. Akrivos, J. Coord. Chem. 65 (2012) 251;
(d) M. Luic, B. Kojic-Prodic, J. Herrema, P.D. Akrivos, P. Karagiannidis, J. Coord. Chem. 34 (1995) 169.

[6] (a) T.S. Lobana, R. Sharma, A. Castineiras, G. Hundal, R.J. Butcher, Inorg. Chim. Acta 362 (2009) 3547;
(b) T.S. Lobana, S. Khanna, A. Castineiras, G. Hundal, Z. Anorg. Allg. Chem. 636 (2010) 454;
(c) T. Shibahara, S. Kobayashi, D. Long, X. Xin, Acta Cryst. C53 (1997) 58.

[7] (a) T.S. Lobana, Rekha, A.P.S. Pannu, G. Hundal, R.J. Butcher, A. Castineiras, Polyhedron 26 (2007) 2621;
(b) T.S. Lobana, R. Sharma, R. Sharma, R.J. Butcher, Z. Anorg. Allg. Chem. 634 (2008) 1785;
(c) S.K. Hadjikakou, C.D. Antoniadis, P. Aslanidis, P.J. Cox, A.C. Tsipis, Eur. J. Inorg. Chem. (2005) 1442.

[8] M.G. Babashkina, D.A. Safin, A. Klein, M. Bolte, Eur. J. Inorg. Chem. 25 (2010) 4018.

[9] D.A. Safin, M.G. Babashkina, M. Bolte, A. Klein, CrystEngComm 13 (2011) 568.

[10] (a) B. Singh, M.G. Drew, G. Kociok-Kohn, K.C. Molloy, N. Singh, Dalton Trans. 40 (2011) 623;
(b) S. Singh, J. Chaturvedi, S. Bhattacharya, Dalton Trans. 41 (2012) 424;
(c) G. Rajput, V. Singh, S.K. Singh, L.B. Prasad, M.G. Drew, N. Singh, Eur. J. Inorg. Chem. (2012) 3885.

[11] P. Aslanidis, S. Kyritsis, M. Lalia-Kantouri, B. Wicher, M. Gdaniec, Polyhedron 48 (2012) 140.

[12] (a) J.-H. Sun, J.-L. Shen, L.-S. Liang, X.-Y. Xu, H.-B. Liu, C.-L. Zhang, Chin. Phys. Lett. 22 (2005) 3176;
(b) K. Kawase, Y. Ogawa, Y. Watanable, H. Inoue, Opt. Express 11 (2003) 2549;
(c) K. Kawase, Opt. Photonics News 15 (2004) 34;
(d) N. Li, J. Shen, J. Sun, L. Liang, X. Xu, M. Lu, Y. Jia, Opt. Express 13 (2005) 6750;
(e) L.G. Francesco, G. Cardini, P.R. Salvi, V. Schettino, J. Phys. Chem. A102 (1998) 2131;
(f) Y.A. Gruzdkov, Y.M. Gupta, J. Phys. Chem. A105 (2001) 6197.

[13] (a) S.-G. Liu, China Basic Sci. 1 (2006) 7;
(b) L.-M. Yang, G.-Z. Zhao, W.-H. Li, Y.-F. Liu, X.-X. Shi, X.-F. Jia, K. Zhao, X.-Y. Lu, Y.-Z. Xu, D.-T. Xie, J.-G. Wu, J.-E. Chen, Spectrochim. Acta 73 (2009) 884;
(c) H.-W. Zhao, M. Ge, W.-F. Wang, Q.-N. Li, X.-H. Yu, Chemistry (in Chinese) 2 (2005) 87;
(d) M. Walther, B. Fischer, M. Schall, H. Helm, P.U. Jepsen, Chem. Phys. Lett. 332 (2000) 389;
(e) A. Markelz, A. Roitberg, E.J. Heilweil, Chem. Phys. Lett. 320 (2000) 42;
(f) V. Krishnakumar, R. Nagalakshmi, Cryst. Growth Des. 8 (2008) 3882;
(g) E.P.J. Parrott, J.A. Zeitler, T. Friščić, M. Pepper, W. Jones, G.M. Day, L.F. Gladden, Cryst. Growth Des. 9 (2009) 1452;
(h) L.-M. Yang, H.-Q. Sun, S.-F. Weng, K. Zhao, L.-L. Zhang, G.-Z. Zhao, Y.-G. Wang, Y.-Z. Xu, X.-Y. Lu, C.-L. Zhang, J.-G. Wu, J.-E. Chen, Spectrochim. Acta 69 (2008) 160;
(i) G.-F. Liu, S.-H. Ma, H.-W. Zhao, T. Ji, Z.-Y. Zhang, W.-F. Wang, J. Mol. Struct. 936 (2009) 56.

[14] (a) C.-L. Ma, Q. Jiang, R.-F. Zhang, Polyhedron 23 (2004) 779;
(b) C.-L. Ma, Q. Jiang, R.-F. Zhang, Appl. Organometall. Chem. 17 (2003) 623.

[15] (a) B.C. Tzeng, G.H. Lee, S.-M. Peng, Inorg. Chem. Comm. 7 (2004) 151;
(b) B.C. Tzeng, Y.-C. Huang, W.-M. Wu, S.Y. Lee, G.H. Lee, S.-M. Peng, Cryst. Growth Des. 4 (2004) 63;
(c) Q. Gao, C.-Y. Zhang, Y. Cui, Y.-B. Xie, Acta Cryst. E65 (2009) m838.

[16] (a) J. Schneider, Young-A. Lee, J. Perez, W.W. Brennessel, C. Flaschenriem, R. Eisenberg, Inorg. Chem. 47 (2008) 957;
(b) I.I. Ozturk, S.K. Hadjikakou, N. Hadjiliadis, N. Kourkoumelis, M. Kubicki, A.J. Tasiopoulos, H. Scleiman, M.M. Barsan, I.S. Butler, J. Balzarini, Inorg. Chem. 48 (2009) 2233.

[17] Y.-H. Jiang, Q.-M. Qiu, R.-X. Jiang, X. Huang, Q.-H. Jin, Acta Cryst. E68 (2012) m1295.

[18] R. Peng, M. Li, D. Li, Coord. Chem. Rev. 254 (2010) 1.

[19] Y. Hu, X.-H. Wang, L.-T. Guo, C.-L. Zhang, H.-B. Liu, X.-C. Zhang, Acta Phys. Sin. (in Chinese) 54 (2005) 4124.

[20] G.M. Sheldrick, SHELXS-97 and SHELXL-97, Software for Crystal Structure Analysis, Siemens Analytical X-ray Instruments Ins, Wisconsin, Madison, USA, 1997.

[21] G.M. Sheldrick, SHELXTL NT Version 5.1. Program for Solution and Refinement of Crystal Structures, University of Göttingen, Germany, 1997.

[22] T.S. Lobana, S. Khanna, G. Hundal, R.J. Butcher, A. Castineiras, Polyhedron 28 (2009) 3899.

[23] T.S. Lobana, S. Khanna, G. Hundal, P. Kaur, B. Thakur, S. Attri, R.J. Butcher, Polyhedron 28 (2009) 1583.

[24] Q.-H. Jin, K.-Y. Hu, L.-L. Song, R. Wang, C.-L. Zhang, X. Zuo, X.-M. Lu, Polyhedron 29 (2010) 441.

[25] T.S. Lobana, A. Castineiras, Polyhedron 21 (2002) 1603.

[26] S.S. Lemos, M.A. Camargo, Z.Z. Cardoso, V.M. Deflon, F.H. Forsterling, A. Hagenbach, Polyhedron 20 (2001) 849.

[27] T.S. Lobano, P.K. Bhatia, E.R.T. Tiekink, J. Chem. Soc. Dalton Trans. (1989) 749.

[28] P. Aslanidis, P.J. Cox, P. Karagiannidis, S.K. Hadjikakou, C.D. Antoniadis, Eur. J. Inorg. Chem. (2002) 2216.

[29] P. Karagiannidis, P. Aslanidis, S. Papastefanou, D. Mentzafos, A. Hountas, A. Terzis, Polyhedron 9 (1990) 981.

[30] K. Singh, J.-R. Long, P. Stavropoulos, J. Am. Chem. Soc. 119 (1997) 2942.

[31] J.-P. Lang, K. Tatsumi, K.-B. Yu, Polyhedron 15 (1996) 2127.

[32] (a) A. Voglerand, H. Kunkely, Coord. Chem. Rev. 230 (2002) 243;
(b) J.T. York, I. Bar-Nahum, W.B. Tolman, Inorg. Chim. Acta 361 (2008) 885.

[33] M.A. Tsiaggali, E.G. Andreadou, A.G. Hatzidimitriou, A.A. Pantazaki, P. Aslanidis, J. Inorg. Biochem. 121 (2013) 121.

[34] P. Aslanidis, P.J. Cox, P. Tsaliki, Polyhedron 27 (2008) 3029.

[35] V. Pawlowsky, G. Knör, C. Lennartz, A. Vogler, Eur. J. Inorg. Chem. (2005) 3167.

[36] A. Tsuboyama, K. Kuge, M. Furugori, S. Okada, M. Hoshino, K. Ueno, Inorg. Chem. 46 (2007) 1992.

[37] Y.-L. Xiao, Q.-H. Jin, Y.-H. Deng, Z.-F. Li, W. Yang, M.-H. Wu, C.-L. Zhang, Chem. Commun. 15 (2012) 146.

[38] Y.-J. Cui, Y.-F. Yue, G.-D. Qian, B.-L. Chen, Chem. Rev. 112 (2012) 1126.

[39] E. Cariati, R. Ugo, F. Cariati, D. Roberto, N. Masciocchi, S. Galli, A. Sironi, Adv. Mater. 13 (2001) 1665.